

pubs.acs.org/Macromolecules Article

Exploring the Effects of Bulky Cations Tethered to Semicrystalline Polymers: The Case of Tetraaminophosphoniums with Ring-Opened Polynorbornenes

Megan Treichel, C. Tyler Womble, Ryan Selhorst, Jamie Gaitor, Taniya M. S. K. Pathiranage, Tomasz Kowalewski,* and Kevin J. T. Noonan*



Cite This: Macromolecules 2020, 53, 8509-8518



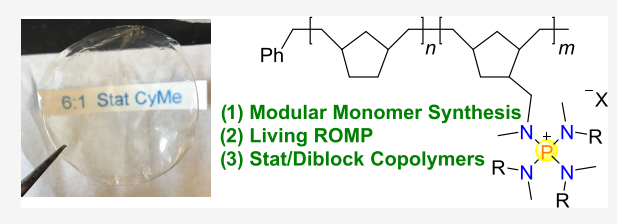
ACCESS

Metrics & More

Article Recommendations

Supporting Information

ABSTRACT: Herein, a simple synthetic method to functionalize norbornene at the 5-position with a base-stable tetraaminophosphonium cation was developed. Upon confirmation that the cationic monomer could be polymerized in a living fashion, statistical and diblock copolymers were synthesized with norbornene as a comonomer. After hydrogenation, the statistical copolymers were effective anion-exchange materials, while the diblock did not produce a free-standing film. Differential scanning calorimetry and atomic force microscopy indicated



that crystallinity was mostly suppressed by the bulky phosphonium cations in the statistical copolymers, with the impact somewhat dependent on the amino groups bound to the phosphorus atom. Small-angle X-ray scattering profiles revealed a two-phase morphology with 3 nm domains arising from ion clustering in the film. Altogether, the study revealed the large impact these novel phosphonium cations have on polymer organization and packing, which is a critical consideration when targeting larger delocalized cations in anion-transport materials.

INTRODUCTION

Materials that enable selective ion transport are critical for a range of applications including redox-flow batteries, fuel cells, ion-exchange membranes, and water treatment. Polymers decorated with ionic groups are a natural choice for these applications as the backbone provides structural integrity and the tethered ionic groups provide pathways for charge movement. A balance of these two phases is needed to maximize membrane stability, material properties, and performance. This balance has become particularly important with hydroxide-based anion-exchange membranes (AEMs).²⁻⁶ A diverse range of polymer backbones and cation combinations have been investigated in AEMs, 2-6 and a number of promising candidates have been identified that rival the performance of proton-exchange membranes. The most compelling aspects that must be addressed with these materials (i.e., ion transport, stability, and membrane characteristics) stimulate questions regarding chain stiffness, polymer architecture, and cation choice. In our work, we are beginning to explore these aspects specifically with hydrocarbon polymers and resonance-stabilized cations to maximize alkaline stability.^{7,8}

Herein, a strategy to synthesize and polymerize a tetraaminophosphonium-functionalized norbornene using ring-opening metathesis polymerization (ROMP) was developed. The phosphonium cation is derived from a well-known class of organic superbases and exhibits exceptional stability to alkaline media. The level of precision that

could be achieved in polymer synthesis prompted us to prepare both block and statistical copolymers of this unit with norbornene as a comonomer. It was anticipated that the semicrystalline hydrogenated ring-opened polynorbornene (hPN) would enhance mechanical integrity and toughness for film formation. Strikingly, the block copolymers were brittle, while statistical copolymers formed free-standing films. Differential scanning calorimetry (DSC), atomic force microscopy (AFM), and small-angle X-ray scattering (SAXS) were used to provide insight into the morphology of the statistical copolymers, while water uptake and conductivity were used to evaluate the AEM performance of these architectures.

RESULTS AND DISCUSSION

Preparation of Polymerizable Phosphonium Salts. Polymers with pendant tetraaminophosphonium cations are more difficult to synthesize than those bearing alkyl and arylphosphoniums. $^{7,8,25-30}$ In the two prior reports on [P- $(NR_2)_4$]+-based polymers, 7,8 a moisture-sensitive trichloro-

Received: February 22, 2020 Revised: July 31, 2020 Published: September 22, 2020





Scheme 1. Synthesis and Polymerization of the Tetraaminophosphonium Monomer

phosphazene ($Cl_3P=NR$) was required as an intermediate during monomer synthesis. Here, a method was developed to simplify the synthesis of polymerizable tetraaminophosphonium salts and broaden the use of these cations in AEMs. A two-step one-pot synthesis of a triaminoiminophosphazene is the key to this approach (Scheme 1A),³¹ with one of the four nitrogen substituents suitable for further derivatization.

The synthesis of the unsymmetrical tetraaminophosphonium was accomplished by the reaction of 3 equiv of N-methylcyclohexylamine with PCl_5 . The resultant triaminochlorophosphonium intermediate was subsequently treated with a slight excess of methylamine. Workup with KPF₆ affords the desired resonance-stabilized cation with a N-H group in a 60% yield. A polymerizable phosphonium salt was then prepared in an 83% yield by alkylation of $[(N(Cy)Me)_3PN-(H)Me][PF_6]$ with a mesyl-substituted norbornene in a two-phase reaction (Scheme 1A). The stereochemistry of the norbornenyl group was critical for polymerization of this monomer, as the endo isomer was markedly less reactive. Given this, a 95% exo norbornene derivative was synthesized according to a literature procedure and employed as the polymerizable group. $^{33-35}$

The CyMe[PF₆] monomer with cyclohexylmethylamino substituents was synthesized first, as this closely resembled the polymerizable tetraaminophosphonium salts reported previously.^{7,8} Other phosphonium derivatives can also be accessed in a straightforward manner using this method. As a representative example, isopropylmethylamine and PCl₅ were used to synthesize an iPrMe[PF₆] norbornene in an identical procedure (Scheme 1A). Tuning cation size and hydrophilicity by altering the amino groups bound to phosphorus will influence morphology, conductivity, and water uptake in AEMs. While tetraaminophosphoniums with cyclohexylmethylamino groups are exceptionally base-stable, 20,21 the cation itself is sterically demanding. Since many other tetraaminophosphoniums are alkaline-stable, 20,21 changing the substituent should serve as a strategy to alter the polymer structure and relevant AEM properties.

Homopolymerization and Copolymerization of Phosphonium Salts. Generally, polymerization of CyMe or iPrMe was possible whether the monomer was paired with either a

PF₆ or a Cl counterion and these were used interchangeably in polymerization. The specific monomer employed is noted in the discussion. Counterion exchange was accomplished using a commercially available exchange resin, and loss of the PF₆⁻ can be visualized using ³¹P{¹H} NMR spectroscopy. Grubbs thirdgeneration catalyst ([(H₂IMes)(Pyr)₂(Cl₂)Ru=CHPh]) was used to polymerize CyMe[Cl] at 22 °C in 1,2-dichloroethane (Scheme 1B).36,37 Upon injection of the monomer into the green catalyst solution, an abrupt color change was observed. H NMR analysis of an aliquot removed from the reaction mixture after 20 min confirmed that the vinyl signal of the monomer at $\delta^{1}H$ 6.1 ppm had disappeared and was replaced with several broad signals upfield corresponding to the polymer at δ^1 H 5.6–5.0 ppm. Gel permeation chromatography (GPC) analysis of the homopolymer^{8,38} revealed a monomodal trace with a narrow molecular weight distribution. This result was a strong indicator that the polymerization proceeded with no termination and a chain extension experiment was then carried out with two sequential additions of CyMe[Cl] to an active polymerization. The elution profiles shifted with each additional monomer feed and provided sufficient evidence that the polymerization was living (Figure 1). Since the homopolymers did not form free-standing films, block copolymers were targeted as they can form high-performing AEMs. 39-55

Norbornene was chosen as the comonomer with CyMe since hydrogenated ring-opened polynorbornene (hPN) is semicrystalline with a $T_{\rm m}$ of 143 °C. ^{23,24} It was anticipated that the copolymerization of norbornene and the phosphonium would be beneficial for achieving good mechanical properties with a 4:1 molar ratio of norbornene: CyMe[PF₆]. The PN block with an active Ru alkylidene chain end was prepared at $-10~{\rm ^{\circ}C}$ using G3 since the low reaction temperature is known to suppress chain transfer. ³⁶ Polymerization of CyMe[PF₆] at lower temperatures was also attempted (between $-20~{\rm and}~0~{\rm ^{\circ}C}$), but the rate of monomer consumption was significantly retarded. Given this, norbornene was polymerized at $-10~{\rm ^{\circ}C}$ over the course of 20 min, and CyMe[PF₆] was then added to the reaction mixture with immediate warming to 22 °C. The copolymerization was quenched with ethyl vinyl ether to afford the vinylidene-terminated diblock copolymer with a near-

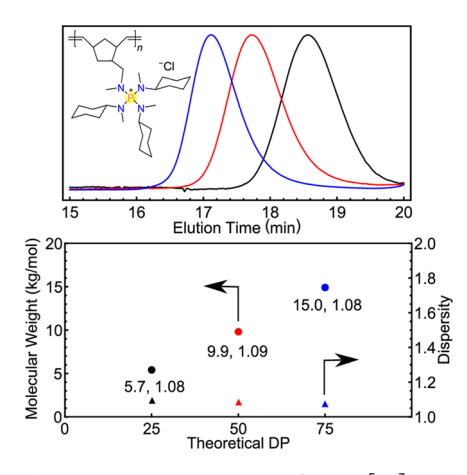


Figure 1. Chain extension experiment of CyMe[Cl] conducted with $[(H_2IMes)(Pyr)_2(Cl_2)Ru=CHPh]$ as the catalyst in 1,2-dichloroethane (0.2 M). Top: GPC traces collected at 40 °C using tetrahydrofuran (THF) as the eluent (with 10 mM LiNTf₂) and molecular weights determined versus polystyrene standards (targeted DPs = 25, 50, 75). Bottom: plot of M_n and molecular weight distribution versus the theoretical DP.

quantitative chain extension (top panel of Figure 2). This material was hydrogenated using tosyl hydrazide (2 equiv) to

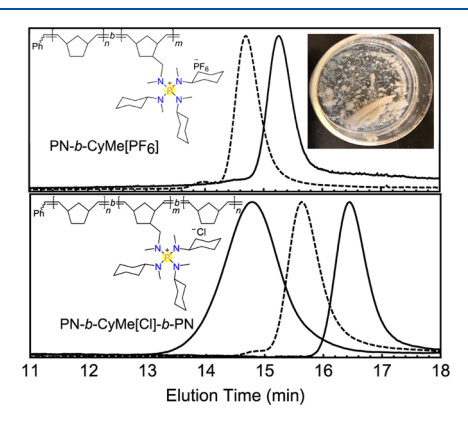


Figure 2. Top: normalized GPC traces of the diblock copolymer from G3 with PN as the first block ($M_{\rm n}=40.1~{\rm kg/mol},~D=1.31$) and CyMe[PF₆] as the second block ($M_{\rm n}=82.8~{\rm kg/mol},~D=1.07$). The inset is a picture of attempts to cast diblock films upon hydrogenation and conversion to the Cl⁻ form. Bottom: normalized GPC traces of the triblock copolymer from G3 with PN as the first block ($M_{\rm n}=31.6~{\rm kg/mol},~D=1.06$), CyMe[Cl] as the midblock ($M_{\rm n}=44.9~{\rm kg/mol},~D=1.21$), and PN as the third and final block ($M_{\rm n}=99.9~{\rm kg/mol},~D=1.16$).

reduce the C=C bonds in the polymer chain. Tetraamino-phosphonium polymers in the PF $_6$ form are not easily exchanged to OH $^-$ upon treatment with aqueous NaOH or KOH. Prior reports on phase-transfer reactions have indicated that counterions play a critical role in the extraction of OH $^-$ into low polarity media. See Given this, the polymer was converted into the Cl $^-$ form for film preparation and eventual exchange to OH $^-$. Upon exchange of the diblock copolymer from the PF $_6$ to Cl $^-$ form, the polymer was solution-cast from hot 1,2-dichlorobenzene in a glass Petri dish above 80 °C. Casting below 80 °C resulted in a turbid solution, which was attributed to the precipitation of the semicrystalline hPN. Unfortunately, hPN-b-CyMe[Cl] did not afford a mechanically stable membrane (picture in the top panel of Figure 2) as

cracks and tears appeared upon attempted removal of the material from the glass dish. An ABA triblock copolymer of norbornene and CyMe[Cl] was then synthesized to flank the ionic chain with insulating blocks and enhance physical crosslinking similar to ABA thermoplastic elastomers. The first PN block was prepared at -10 °C, with chain extension of the CyMe midblock at 22 °C. The third PN end block was prepared at 22 °C to ensure that no issues arose from initiation with the CyMe chain end, which did result in a slightly broader distribution (bottom panel of Figure 2). After hydrogenation, the hPN-b-CyMe[Cl]-b-hPN was also solvent-cast from 1,2dichlorobenzene above 80 °C. In contrast to the diblock, the triblock could be removed from the dish as a delicate freestanding film upon hydration. However, upon conversion to hPN-b-CyMe[OH]-b-hPN, the polymer lost integrity similar to the diblock, and conductivity measurements could not be completed. The film did not swell excessively but was sensitive to minor shear forces, which led to the material breakdown. Changing the molar ratio of comonomers or replacing CyMe with iPrMe did not result in major improvements.

Statistical copolymers were then synthesized in an effort to improve ductility of the final copolymer (Table 1). At least 5 molar equiv of norbornene relative to CyMe[PF₆] and iPrMe[PF₆] was needed to form AEMs, which did not swell excessively in water. Tosyl hydrazide (~2 equiv/double bond) was used to hydrogenate the C=C bonds in these copolymers (Supporting Information). Between 90 and 98% of the double bonds were reduced using this method, with residual double bonds observed at low intensities in the ¹H NMR spectra of the final copolymer.

NMR Spectroscopy. The microstructure of the statistical copolymers was difficult to probe from kinetic analysis of the reaction. Aliquots removed from the polymerization after only 30 s revealed that monomer consumption was ~95% complete. Attempts to lower the reaction temperature for a more indepth study disproportionately impacted the polymerization rate of the bulkier phosphonium monomer. Though the arrangement of monomer residues along the chain was not established, the final incorporation of the phosphonium salt was estimated from ¹H NMR spectroscopy. The N-Me groups bound to the phosphonium appear between δ 2.5 and 3 ppm. These were compared to the entire aliphatic region of the sample between δ 2.2 and 0.5 ppm. In nearly all cases, the integration of the aliphatic portion tended to be a little lower than expected but consistently within 5-10% of the target value. For example, in 6:1 hPN-co-iPrMe[Cl] as shown in Figure 3, the ratio of N-Me groups to the aliphatic region should theoretically be 12:100 with a 12:91 ratio observed.

The stereochemical possibilities for ring-opened polynor-bornenes have been well documented. The central methylene signal of the cyclopentyl ring is split into several signals from the potential dyad configurations of the ring along the backbone. This signal in the synthesized phosphonium copolymers indicated that the chain was atactic, with ratios of $\sim\!1\!:\!2\!:\!1$ for the mm/mr/rr signals. The methyl and methylene resonances of the amino group connecting the polymer and the cation are broad and difficult to observe in one-dimensional (1D) 13 C NMR experiments, likely due to the restricted rotation from the bulky cation. Some unexpected fine structure and splitting were also observed in the 31 P NMR spectra for hPN-co-CyMe[Cl] and hPN-co-iPrMe[Cl] between δ^{31} P 44 and 47 ppm (Figures S20 and S24). We considered whether the rotational restriction or poor solvation led to this more

Table 1. Statistical Copolymerization of Phosphonium with Norbornene and the Relevant AEM Properties of the Final Copolymers

entry	copolymer (monomer ratio)	$M_{\rm n}$ (\mathcal{D}) (kg/mol)	$IEC_{theo} (mmol/g)$	IEC" (mmol/g)	WU ^o OH ⁻ (%)	$\sigma_{25^{\circ}C}$ OH ⁻ (mS/cm)	$\sigma_{80^{\circ}\text{C}}$ OH ⁻ (mS/cm)
1	PE-co-CyMe ^{d} (5:1)		0.9	0.7	52	22 ± 1	
2	hPN-co-CyMe (5:1)	99 (1.21)	1.0	0.99	82	19 ± 2	
3	hPN-co-CyMe (6:1)	93 (1.20)	0.9	0.9	52	18 ± 2	
4	hPN-co-iPrMe (5:1)	87 (1.30)	1.1	0.78	86	27 ± 1	43 ± 3
5	hPN-co-iPrMe (6:1)	106 (1.25)	1.0	0.99	75	22 ± 1	40 ± 3

"Ion-exchange capacity (IEC) was measured using back-titration. ^bWater uptake (WU) was determined gravimetrically for each film in the OH⁻ form. ^cConductivity was determined using electrochemical impedance spectroscopy with the reported values as an average of three trials except entry 2. Errors refer to the standard deviation of the sample set. ^dData were taken from ref 7.

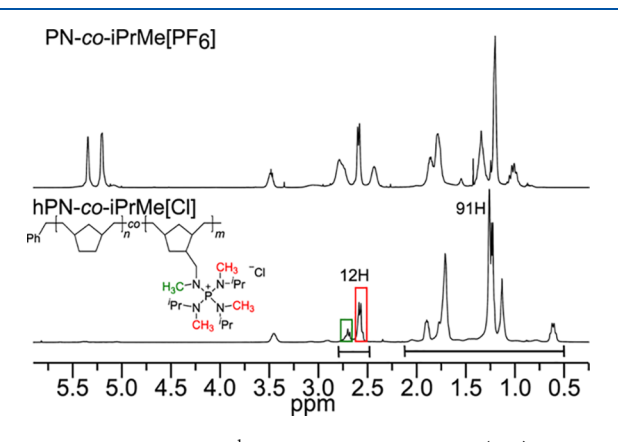


Figure 3. Representative ¹H NMR spectra before (top) and after (bottom) hydrogenation of 6:1 PN-co-iPrMe. The top spectrum was collected in CDCl₃ at 22 °C and the bottom spectrum was collected in tetrachloroethane- d_2 at 22 °C.

complicated pattern, but NMR spectra recorded at 80 $^{\circ}$ C in 1,1,2,2-tetrachloroethane- d_2 or with methanol as a cosolvent did not alter the observed spectrum. At this time, it is difficult to explicitly determine whether the unusual splitting pattern arises from restricted rotation, poor solvation or tacticity.

Physical Characterization of the Statistical Copolymers. The statistical copolymers were characterized using DSC and AFM with comparison to the hPN homopolymer. The melt transition of hPN appears at 143.8 °C ($\Delta H_{\rm m} = 58~{\rm J/g}$) in the DSC trace as expected (Figure 4, top left), ^{23,24} and the AFM height image displays the characteristic spherulites of a semicrystalline polymer (Figure 4, bottom left). The two statistical copolymers produced markedly different DSC traces than the homopolymer, with 5:1 hPN-co-CyMe[Cl] displaying essentially no crystallinity, while a weak transition ($\Delta H_{\rm m} = 5.9~{\rm J/g}$) was observed in 5:1 hPN-co-iPrMe[Cl] (middle and right in Figure 4). The melt transition depression relative to the homopolymer was attributed to the statistical nature of the copolymers. By weight, the iPrMecopolymer retained ~20% of the crystallinity of the homopolymer (as the copolymer is ~50% norbornene by weight). The DSC traces for the 6:1

hPN-co-CyMe[Cl] and hPN-co-iPrMe[Cl] are nearly identical to the 5:1 variants, with minimal crystallinity in the CyMe sample and a minor transition for the iPrMe sample ($\Delta H_{\rm m} = 5.3~{\rm J/g}$). No hints of the lamellae are observed in an annealed film of hPN-co-CyMe[Cl], while some are observable in hPN-co-iPrMe[Cl], consistent with the DSC patterns. The bulkier cation with the cyclohexylmethylamino substituents has a somewhat larger impact on crystallinity and chain packing, which is not surprising given its larger dimensions. DSC traces of both statistical copolymers cast from chlorinated solvents display different patterns than the annealed forms, suggesting that solvent casting can impact morphology in these materials.

SAXS analysis of the solvent-cast films in the dry state (Clform) provided further insight into the organization of these materials. The patterns observed in the SAXS profiles for hPN-co-CyMe[Cl] (both 5 and 6:1) suggest some degree of phase separation at the 30 nm length scale (arrows in Figure 5A,B). One can envision that such phase separation could arise from the systematic variation of the copolymer composition along the backbone caused by the different reactivities of the two monomers, with bulkier (thus less reactive) segments being incorporated more frequently at the later stages of polymerization. Kinetic studies to confirm this hypothesis about the origin of phase separation were not conclusive due to the fast polymerization rates of both monomers at 22 °C. Interestingly, no phase separation at this length scale was observed in the iPrMe copolymers containing less bulky ionic groups (Figure 5C,D).

Closer inspection of the high q range of SAXS patterns of both sets of copolymers revealed the presence of a distinct change of slope in the 3 nm range. We attribute this feature to the local aggregation of sequences of hPN segments frustrated by the statistically distributed ionomeric groups. An hPN chain with the ethylene units in a zig-zag conformation and the rings in an envelope conformation affords a repeat unit length of \sim 5 Å.²³ The observed 3 nm length scale is therefore comparable with the average length of hPN runs between phosphonium-bearing segments (\sim 5–6 norbornenes per phosphonium). This assignment is further supported by the absence of \sim 3 nm clustering in the triblock copolymer hPN-b-CyMe[Cl]-b-hPN

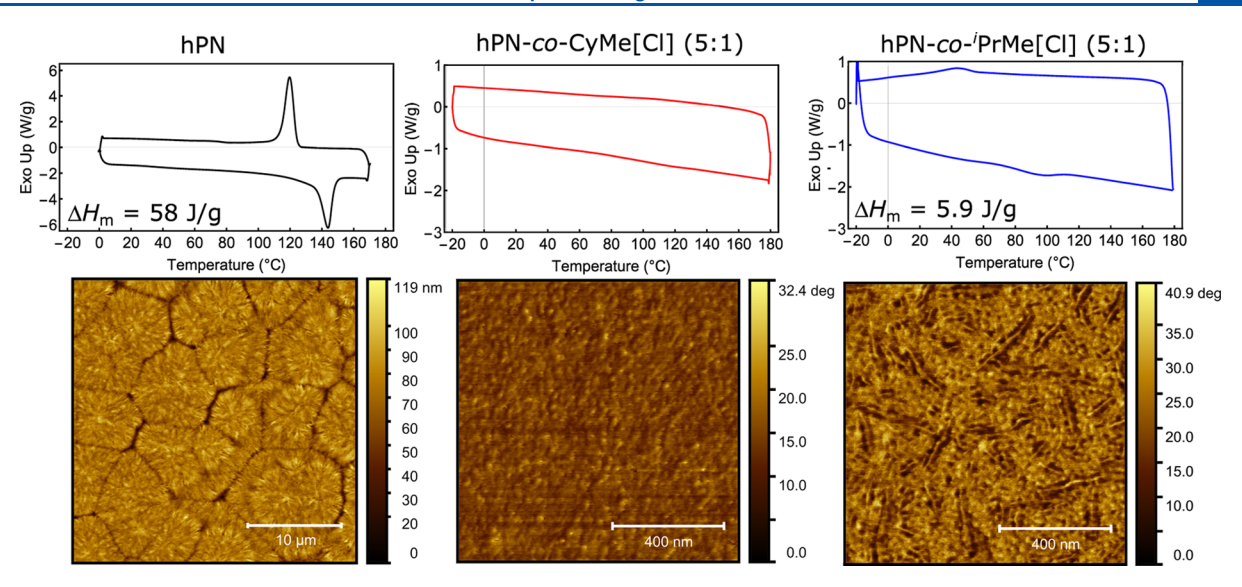


Figure 4. Top: differential scanning calorimetry traces (second run) measured at a heating rate of $10 \,^{\circ}$ C/min for the hPN homopolymer in black, and the statistical copolymers hPN-co-CyMe (5:1) (red) and hPN-co- i PrMe (5:1) (blue). Bottom: the corresponding AFM images of thin films were collected through a heating and rapid quench into liquid nitrogen. The homopolymer image was collected in contact mode and is a height image (inset, scale bar $10 \, \mu$ m), while the copolymers were measured in tapping mode with phase images being shown (inset, scale bar $400 \, \text{nm}$).

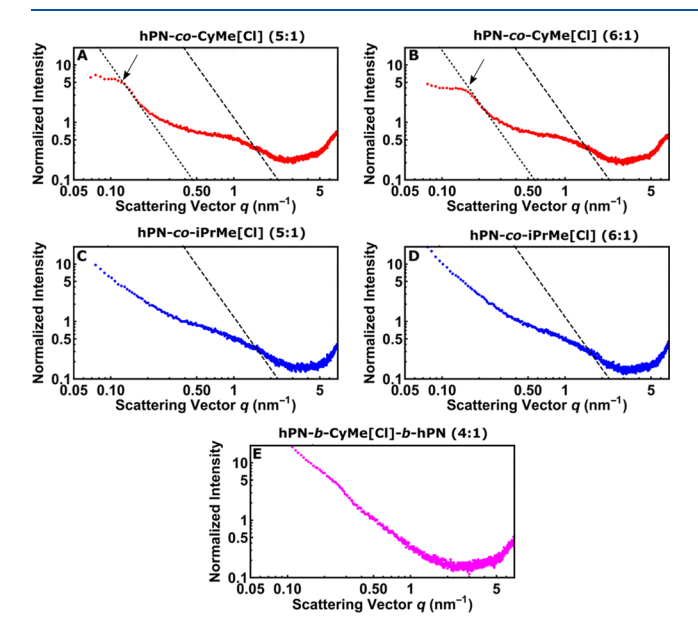


Figure 5. SAXS profiles acquired for the various copolymer films collected at 22 $^{\circ}$ C. The dashed lines are ideal q⁻³ scaling, to indicate deviations from ideal behavior for the tall narrow-slit X-ray beam collimation used in this study. ⁵⁹ The change in slope indicates that boundaries between the two phase-separated regions are more diffuse.

(Figure 5E). Interestingly, the hPN-b-CyMe[Cl]-b-hPN copolymer exhibited only an ill-defined feature at the 30 nm length scale. This suggests that the formation of well-defined nanoscale morphology due to the phase separation between the blocks was suppressed by kinetic trapping due to the crystallization of the hPN block.

lonic Properties of the Statistical Copolymers. The hPN-co-CyMe[Cl] and hPN-co-iPrMe[Cl] were solvent-cast at 80 °C from either 1,1,2,2-tetrachloroethane (TCE) or 1,2-dichlorobenzene to form free-standing films. The as-cast copolymer films were exchanged to the OH⁻ form using a 1 M KOH or NaOH solution (Table 1), and IEC values were determined using standard back-titration, while water uptakes

were determined gravimetrically. Hydroxide conductivity was measured using electrochemical impedance spectroscopy (EIS) conducted on thin films in liquid water (four-point probe geometry). The experimental IEC values for all of the synthesized polymers ranged between 0.9 and 1.1 mmol/g and were quite close to the theoretical values, as expected. Slightly larger water uptakes were noted across the series compared to a previously synthesized polyethylene-based tetraaminophosphonium copolymer (entry 1, Table 1), but generally, the ring-opened norbornene copolymers were similar to the synthesized PE derivative (Table 1).

The 5:1 and 6:1 copolymers of hPN-co-iPrMe[OH] were slightly more conductive than the comparable hPN-co-CyMe[OH] copolymers at room temperature (Table 1). This was attributed to the slight differences in IECs of the two materials, along with the morphology differences as evidenced by AFM and SAXS. Comparison of the two types of copolymers at 80 °C produced more stark contrast, as the hPN-co-CyMe[OH] films lost their mechanical integrity at this temperature, which made it impossible to obtain reliable conductivity values. By contrast, the hPN-co-iPrMe[OH] could be measured repeatedly at 80 °C and this material is the most conductive tetraaminophosphonium polymer measured to date (Table 1). DSC, AFM, and SAXS all suggest that the iPrMe cation has a lower impact on hPN organization, which is attributed to the lower steric constraints of this cationic moiety. This observation highlights the importance of the amino groups bound to phosphorus and the critical impact of this moiety on the transport properties and mechanical stability of tetraaminophosphonium-based AEMs. It has prompted consideration of other types of phosphonium units, which may have a lower impact on hPN organization to further improve conductivity, so cation concentration can be increased along the backbone.

CONCLUSIONS

In conclusion, we have developed a facile synthesis to prepare a modular triaminoiminophosphazene. This precursor can be then attached to norbornene in a straightforward substitution

reaction. Phosphonium-functionalized norbornenes were then polymerized in a living fashion using the Grubbs third-generation catalyst. Well-defined AB and ABA block copolymers were prepared by sequential monomer addition with norbornene, but these materials did not form the free-standing films necessary to produce AEMs. Statistical copolymers by contrast afforded flexible OH⁻ conducting membranes. The amino groups bound to phosphorus had an impact on morphology, mechanical integrity, and ionic transport in these materials, which will be explored in more detail in the future. The facile synthesis of these phosphonium cations should enable a wide range of follow-up work with alternative comonomers and sterically less demanding phosphonium cations to optimize transport properties while retaining chemical stability.

EXPERIMENTAL SECTION

Materials and Methods. Nearly all reactions were carried out under N₂, but manipulations of compounds and polymers were carried out in air unless otherwise specified. All reagents and solvents were purchased from commercial sources and used as received unless otherwise specified. Grubbs' third-generation initiator (G3), [(H₂IMes)(pyr)₂(Cl)₂Ru=CHPh], was prepared according to a published report.⁶⁰ The ((1R₂S₃AR)-bicyclo[2.2.1]hept-5-en-2-yl)methanol was synthesized according to a literature procedure.³³

NMR Analysis. All NMR spectra were recorded on a 500 MHz Bruker Avance 3 Spectrometer or a 500 MHz Bruker Neo Spectrometer with Prodigy Cryoprobe. The ^1H NMR spectra were referenced to residual protio solvents (7.26 ppm for CHCl₃, 2.50 ppm for DMSO- d_6 , and 6.00 ppm for TCE- d_2), and ^{13}C NMR were referenced to the solvent signal (CDCl₃: 77.16 ppm, DMSO- d_6 : 39.52, TCE- d_2 : 73.78 ppm). The $^{31}\text{P}\{^1\text{H}\}$ NMR spectra were electronically referenced using internal Bruker software according to a universal scale determined from the precise ratio, Ξ , of the resonance frequency of the ^{31}P nuclide to the ^{1}H resonance of tetramethylsilane (TMS) in a dilute solution (φ <1%). Minor signals attributed to the endo isomer are observed in the NMR spectra for ((1 R_2 2 S_1 4R)-bicyclo[2.2.1]hept-5-en-2-yl)methyl methanesulfonate, but are not included in the reported shifts.

High-Resolution Mass Spectrometry (HRMS). ESI-MS was performed on a Thermofisher Exactive EMR spectrometer operating with the XCalibur software (Version 4.1). Data were recorded continuously with a scanned mass range of 150–600 m/z using a spray voltage of 4.2 kV, a capillary temperature of 275 °C, and a nitrogen sheath gas flow rate of 20.

Gel Permeation Chromatography. GPC measurements were performed on a Waters Instrument equipped with a 2690 autosampler, a Waters 2414 refractive index (RI) detector, and two SDV columns (porosities 1000 and 100 000 Å; Polymer Standard Services). The eluent (THF) was doped with 10 mM lithium bis(trifluoromethanesulfonyl)imide (flow rate of 1 mL/min, 40 °C). A 9-point calibration based on polystyrene standards (Polystyrene, ReadyCal Kit, Polymer Standard Services) was applied for determination of molecular weights. All polymer aliquots subjected to GPC analysis were prepared by quenching ~0.1 mL of the polymer solution with 0.1 mL of ethyl vinyl ether in 1 mL of chlorobenzene. The solution was concentrated and dissolved in 2 mL of THF and filtered through a 0.22 μm polytetrafluoroethylene (PTFE) syringe filter and analyzed.

lon-Exchange Capacity. IEC was measured using standard backtitration methods. The thin film membrane in the Cl⁻ form was added to 100 mL of 1 M KOH in a Nalgene bottle for 17 h. The KOH solution was quickly decanted from the membrane and 25 mL of fresh deionized water was added. After soaking for 20 min, the solution was quickly decanted and replaced with another fresh portion of deionized water. This process was repeated a total of three times. The solution was decanted from the membrane and replaced with 25 mL of standardized 0.1 N HCl solution for 17 h. The remaining acidic

solution was titrated with standardized 0.1 N NaOH using an Accumet AB15 pH Meter, and the volume used to obtain pH = 7 was recorded. A control titration of 25 mL of standardized 0.1 N HCl was done using standardized 0.1 N NaOH, and the volume used to obtain pH = 7 was recorded. The difference in volume between the control titration and the membrane titration was used to calculate the IEC using the following equation

$$(V_{\text{control}} - V_{\text{membrane}}) \times \frac{0.1 \text{ mmol NaOH}}{1 \text{ mL solution}} / \text{membrane weight}$$

$$= \text{IEC (mmol/g)}$$

Differential Scanning Calorimetry (DSC) and Thermal Gravimetric Analysis (TGA). DSC analysis was performed on a TA Instruments DSC Q20. Samples were scanned from 0 to 180 °C at a rate of 10 °C/min under N_2 for two cycles. TGA was performed using a Perkin Elmer Pyris under a N_2 atmosphere. Samples were heated from 50 to 800 °C at a rate of 10 °C/min.

Atomic Force Microscopy. The hPN homopolymer was dissolved in hot TCE (above 120 °C) and filtered through a 0.22 µm PTFE syringe filter onto a silicon wafer. The solvent was evaporated, and the sample was analyzed. The 5:1 phosphonium copolymers were also dissolved in TCE, filtered through a 0.22 μm PTFE syringe filter and cast onto silicon wafers. The solvent was evaporated, and then the samples were heated above 150 °C, at which time they were submerged directly in liquid nitrogen for analysis. All imaging was performed using Dimension 3000 system with a Nanoscope V controller (Veeco, currently Bruker, Inc). Statistical copolymer images were acquired in tapping mode using silicon cantilevers with a nominal spring constant of 35 N/m and resonance frequency of 190 kHz. Imaging was carried out at a frequency at which the cantilever amplitude was equal to 85% of its amplitude onresonance and generated the signal of 250 mV, which typically required drive amplitude of 42-68 mV. The typical values of set-point ranged from 160-200 mV. Images of the hPN homopolymer were collected in contact mode using low spring constant silicon nitride probes. All AFM images were rendered using Gwyddion 2.56 Software.

Small-Angle X-ray Scattering. SAXS was performed on polymer films using an Anton Paar SAXSess mc2 with beam collimation. Cu $K\alpha$ radiation at 1.542 Å was used as the X-ray source. X-ray source was operated at 40 kV and 50 mA. Experiments were carried out under vacuum (1–2 mbar) at room temperature, with acquisition times of 180 s averaged over 1 frame. Blank samples were taken at the same acquisition time and frames to provide a background for subtraction.

Conductivity. Conductivity was measured by four-probe electrochemical impedance spectroscopy (EIS) using a Scribner Membrane Conductivity Clamp and a Bio-Logic SP-150 Potentiostat. The thin film membrane in the Cl $^-$ form was cut to dimensions of ${\sim}20~\text{mm}\times5$ mm. Membrane strips were soaked in 100 mL of 1 M KOH or NaOH in a Nalgene bottle for 17 h. The KOH solution was quickly decanted from the bottle, and 100 mL of fresh deionized water was added. After soaking for 20 min, the solution was quickly decanted and replaced with another fresh portion of deionized water. This process was repeated a total of three times. The thin film membrane, now in the OH- form, was quickly assembled in the conductivity clamp and submerged in fresh deionized water at 25 °C to avoid conversion of OH- to carbonates. EIS was performed by applying a sinusoidal (alternating current, AC) voltage of 10 mV across the membrane sample at frequencies between 400 kHz and 0.1 Hz (scanning from high to low frequency) and measuring the current response. The impedance value with the lowest imaginary response at the highest frequency was then used to calculate hydroxide conductivity through the following formula

$$\sigma = \frac{L}{Z'WT}$$

where L is the length between the sense electrodes (0.425 cm), Z^{\prime} is the real impedance, W is the membrane width, and T is the

membrane thickness as measured with a digital micrometer. To directly compare different membrane strips, Nyquist plots of specific impedance were graphed by normalizing the real and imaginary impedances through the following equations (Supporting Information)

specific
$$Z' = \frac{Z'WT}{L}$$
, specific $Z'' = \frac{Z''WT}{L}$

Tris(cyclohexyl(methyl)amino)(methylamino)phosphonium Hexafluorophosphate(V). A 500 mL Schlenk flask under a N2 atmosphere equipped with an addition funnel was charged with chlorobenzene (250 mL) and solid PCl₅ (12.3 g, 59 mmol). The flask was cooled to 0 °C using an ice water bath. N-Methylcyclohexylamine (23 mL, 176 mmol) was added dropwise over a period of 10 min, and then triethylamine (32.8 mL, 235 mmol) was added dropwise over a period of 10 min. The reaction mixture was warmed to room temperature and stirred for 17 h. An aliquot was removed and analyzed using ³¹P{¹H} NMR spectroscopy to ensure complete conversion to the desired product ($\delta \sim 51$ ppm). Then, 35.5 mL of a methylamine solution (71 mmol, 2.0 M in THF) was added and the flask was heated to 55 °C using an oil bath. The mixture was stirred for 17 h, and another aliquot was removed and analyzed using $^{31}P\{^{1}H\}$ NMR spectroscopy to ensure complete conversion to the final product ($\delta \sim 41$ ppm). The reaction mixture was filtered to remove any ammonium salts, and the filtrate was concentrated in vacuo at 80 °C. The crude oil was diluted with 200 mL of CH2Cl2 and transferred to a separatory funnel. The organic solution was washed twice with a saturated KPF₆ solution (2 × 150 mL) and once with water (100 mL). The organic layer was subsequently dried over anhydrous sodium sulfate and concentrated using rotary evaporation. The crude oil was diluted with 10 mL of CH₂Cl₂ and was precipitated into 500 mL of diethyl ether. The white solid was collected using vacuum filtration and used without further purification (19.1 g, 60% yield). ¹H NMR (500 MHz, DMSO- d_6) δ 5.61–5.50 (m, 1H), 3.08– 2.96 (m, 3H), 2.57 (d, J_{PH} = 10.0 Hz, 9H), 2.53 (dd, J_{PH} = 12.7, J_{HH} = 5.5 Hz, 3H), 1.83–1.75 (m, 6H), 1.70–1.49 (m, 15H), 1.34–1.22 (m, 6H), 1.13–1.00 (m, 3H). 13 C{ 1 H} NMR (126 MHz, DMSO- 1 d₆) δ 54.7 (d, J_{PC} = 5.1 Hz), 29.9 (d, J_{PC} = 2.9 Hz), 28.6 (d, J_{PC} = 3.9 Hz), 27.6, 25.4, 24.7. $^{31}P\{^{1}H\}$ NMR (202 MHz, DMSO- d_6) δ 41.4, -144.2 (sep, $J_{PF} = 713 \text{ Hz}$). HRMS (ESI): [M]⁺ calcd for $C_{22}H_{46}N_4P^+$, 397.3455; found, 397.346.

Tris(isopropyl(methyl)amino)(methylamino)phosphonium Hexafluorophosphate(V). A 500 mL Schlenk flask under a N₂ atmosphere equipped with an addition funnel was charged with chlorobenzene (200 mL) and solid PCl₅ (10.0 g, 48 mmol). The flask was cooled to 0 °C using an ice water bath. N-Isopropylmethylamine (15 mL, 144 mmol) was added dropwise over a period of 10 min, and then triethylamine (26.8 mL, 192 mmol) was added dropwise over a period of 10 min. The reaction mixture was warmed to room temperature and stirred for 17 h. An aliquot was removed and analyzed using ³¹P{¹H} NMR spectroscopy to ensure complete conversion to the desired product ($\delta \sim 51$ ppm). Methylamine solution (28.8 mL, 58 mmol, 2.0 M in THF) was added, and the flask was heated to 55 °C using an oil bath. The mixture was stirred for 17 h, and another aliquot was removed and analyzed using ³¹P{¹H} NMR spectroscopy to ensure complete conversion to the desired product ($\delta \sim 41$ ppm). The reaction mixture was filtered to remove any ammonium salts, and the filtrate was concentrated in vacuo at 80 °C. The crude oil was diluted with 200 mL of CH₂Cl₂ and transferred to a separatory funnel. The organic solution was washed twice with a saturated KPF₆ solution (2 × 150 mL) and once with water (100 mL). The organic layer was subsequently dried over anhydrous sodium sulfate and concentrated using rotary evaporation. The crude oil was diluted with 10 mL of CH2Cl2 and was precipitated into 500 mL of diethyl ether. The white solid was collected using vacuum filtration and used without further purification (9.7 g, 48% yield). ¹H NMR (500 MHz, CDCl₃) δ 3.75 (br s, 1H), 3.59 (dddd, J = 12.2, 9.5, 7.2, 6.1 Hz, 3H), 2.67 (dd, J = 12.2, 5.6 Hz, 3H), 2.60 (d, J = 9.9 Hz, 9H), 1.20 (d, J = 6.7, 18H). ¹³C{¹H} NMR (126 MHz, CDCl₃) δ 47.1 (d, J_{PC} = 5.7 Hz), 28.4 (d, J_{PC} = 1.4 Hz), 27.6 (d, J_{PC} = 4.2 Hz),

20.2 (d, J_{PC} = 3.3 Hz). $^{31}P\{^{1}H\}$ NMR (202 MHz, CDCl₃) δ 40.7, -144.4 (sep, J_{PF} = 712 Hz). HRMS (ESI): [M]⁺ calcd for $C_{13}H_{34}N_{4}P^{+}$, 277.2516; found, 277.252.

((1R,2S,4R)-Bicyclo[2.2.1]hept-5-en-2-yl)methyl Methanesulfonate. A 100 mL Schlenk flask was charged with CH₂Cl₂ (50 mL), ((1R,2S,4R)-bicyclo[2.2.1]hept-5-en-2-yl)methanol (4.7 g, 38 mmol), and pyridine (6.1 mL, 76 mmol), and the contents were placed under a N2 atmosphere. The flask was cooled to 0 °C using an ice water bath. Methanesulfonyl chloride (4.4 mL, 57 mmol) was added dropwise, and then the reaction mixture was gradually warmed to 22 °C and stirred for 17 h. The contents of the flask were filtered, and the filtrate was diluted with \sim 50 mL of diethyl ether and \sim 50 mL of water. The organic solution was washed with a 1 M HCl solution $(5 \times 50 \text{ mL})$, twice with a 5% w/w NaHCO₃ solution $(2 \times 50 \text{ mL})$, and once with water (50 mL). The organic solution was subsequently dried over anhydrous sodium sulfate and concentrated using rotary evaporation to produce an orange oil. The crude oil was purified through a short silica plug using diethyl ether and concentrated through rotary evaporation to produce a yellow-orange oil (6.3 g, 83% yield). ¹H NMR (500 MHz, CDCl₃) δ 6.08 (t, J_{HH} = 1.9 Hz, 2H), 4.26 (dd, $J_{HH} = 9.7$, 6.5 Hz, 1H), 4.09 (t, $J_{HH} = 9.4$ Hz, 1H), 3.00 (s, 3H), 2.87-2.84 (m, 1H), 2.79-2.75 (m, 1H), 1.84-1.76 (m, 1H), 1.43–1.34 (m, 1H), 1.33–1.25 (m, 2H), 1.21–1.12 (m, 1H). ¹³C NMR (126 MHz, CDCl₃) δ 137.2, 136.0, 73.9, 45.0, 43.5, 41.7, 38.5, 37.4, 29.5.

((Bicyclo[2.2.1]hept-5-en-2-ylmethyl)(methyl)amino) Tris-(cyclohexyl(methyl)amino)phosphonium Hexafluorophosphate(V) (CyMe[PF₆]). Tris(cyclohexyl(methyl)amino) (methylamino) phosphonium hexafluorophosphate (V) (3.8 g, 7.0 mmol), chlorobenzene (4 mL), 8 g of 50% (w/w) KOH_{ao}, and ((1R,2S,4R)-bicyclo[2.2.1]hept-5-en-2-yl)methyl methanesulfonate (2.2 g, 10.9 mmol) were added to a 25 mL flask. The flask was placed in a 100 °C oil bath, and the reaction mixture was stirred for 24 h. An aliquot from the organic layer was removed and analyzed by ³¹P{¹H} NMR spectroscopy to ensure complete conversion to the desired product ($\delta \sim 45$ ppm). The flask was cooled, and the mixture was transferred to a separatory funnel where it was diluted with 50 mL of water and 50 mL of CH₂Cl₂. The organic layer was separated, the aqueous layer was extracted with CH₂Cl₂ (2 × 50 mL), and the organic layers were combined and washed with a saturated KPF₆ solution (3 × 50 mL) and once with water (50 mL). The combined organic layers were dried over anhydrous sodium sulfate and then concentrated using rotary evaporation. The crude oil was precipitated into 200 mL of diethyl ether, and the solids were collected using vacuum filtration. The product was isolated as a white powder (3.7 g, 83% yield). Full characterization of the monomer was completed after exchange to the Cl⁻ form using an anion-exhange resin as described below. H NMR (500 MHz, CDCl₃) δ 6.10–6.04 (m, 2H), 3.06–2.92 (m, 5H), 2.87 (s, 1H), 2.80 (d, $J_{PH} = 9.9$ Hz, 3H), 2.65 (d, $J_{PH} = 9.8$ Hz, 9H), 2.54 (s, 1H), 1.91-1.83 (m, 6H), 1.72-1.60 (m, 10H), 1.59-1.50 (m, 6H), 1.43-1.38 (m, 1H), 1.37-1.30 (m, 1H), 1.30-1.18 (m, 6H), 1.18-1.00 (m, 5H). ¹³C{¹H} NMR (126 MHz, CDCl₃) δ 137.4, 135.9, 56.0 (d, J_{PC} = 4.9 Hz), 54.8 (d, J_{PC} = 4.2 Hz), 45.6, 45.3, 41.9, 38.2 (d, J_{PC} = 3.6 Hz), 36.6 (d, J_{PC} = 3.5 Hz), 32.0, 30.6 (t, J_{PC} = 3.1 Hz), 30.3 (d, J_{PC} = 3.8 Hz), 26.1, 25.0. $^{31}P\{^{1}H\}$ NMR (202 MHz, CDCl₃) δ 46.7.. HRMS (ESI): [M]⁺ calcd for C₃₀H₅₆N₄P⁺, 503.4237; found, 503.424.

((Bicyclo[2.2.1]hept-5-en-2-ylmethyl)(methyl)amino) Tris-(is o p r o p y l (m e t h y l) a m i n o) p h o s p h o n i u m Hexafluorophosphate(V) ('PrMe[PF₆]). Tris(isopropyl(methyl)amino)(methylamino)phosphonium hexafluorophosphate(V) (2.58 g, 6.1 mmol), chlorobenzene (5 mL), 10 g of 50% (w/w) KOH_{aq}, and ((1R,2S,4R)-bicyclo[2.2.1]hept-5-en-2-yl)methyl methanesulfonate (2.0 g, 9.9 mmol) were added to a 25 mL flask. The flask was placed in an oil bath set at 100 °C, and the reaction mixture was stirred for 24 h. An aliquot from the organic layer was removed and analyzed by 31 P{ 1 H} NMR spectroscopy to ensure complete conversion to the desired product (δ ~ 45–46 ppm). The flask was cooled, and the mixture was transferred to a separatory funnel where it was diluted with 50 mL of water and 50 mL of CH₂Cl₂. The organic

Macromolecules Article pubs.acs.org/Macromolecules

layer was separated, the aqueous layer was extracted with CH₂Cl₂ (2 × 50 mL), and the organic layers were combined and washed with a saturated KPF₆ solution (3 \times 50 mL) and once with water (50 mL). The combined organic layers were dried over anhydrous sodium sulfate and then concentrated using rotary evaporation. The crude oil was precipitated into 200 mL of diethyl ether, and the solids were collected using vacuum filtration. The product was isolated as a white powder (2.7 g, 84% yield). ¹H NMR (500 MHz, CDCl₃) δ 6.13–6.08 (m, 2H), 3.60–3.44 (m, 3H), 3.05–2.91 (m, 2H), 2.90 (s, 1H), 2.78 (d, J_{PH} = 10.1 Hz, 3H), 2.62 (d, J_{PH} = 9.8 Hz, 9H), 2.60 (s, 1H), 1.69 (qd, *J* = 7.6, 4.1 Hz, 1H), 1.42 (dt, *J* = 8.9, 1.9 Hz, 1H), 1.37 (ddd, *J* = 11.3, 8.3, 2.5 Hz, 1H), 1.23 (d, *J* = 6.6 Hz, 18H), 1.21–1.16 (m, 2H). ¹³C{¹H} NMR (126 MHz, CDCl₃) δ 137.3, 136.1, 54.3 (d, J_{PC} = 4.1 Hz), 47.3 (d, J_{PC} = 5.7 Hz), 45.7, 45.4, 42.0, 38.1 (d, J_{PC} = 4.3 Hz), 36.2 (d, J_{PC} = 3.7 Hz), 32.0, 28.6 (d, J_{PC} = 3.6 Hz), 20.1 (t, J_{PC} = 3.2 Hz). $^{31}P\{^{1}H\}$ NMR (202 MHz, CDCl₃) δ 45.0, -144.4 (sep, J_{PF} = 712 Hz). HRMS (ESI): [M]⁺ calcd for C₂₁H₄₄N₄P⁺, 383.3298; found,

Anion Exchange of Phos $[PF_6]$ to Phos[CI] Using an Amberlite IRA-400 CI^- Exchange Resin. Either $CyMe[PF_6]$ or iPrMe[PF₆] (1.0 g) was dissolved in 50 mL of a methanol/acetone solution (75% v/v), and 8 g of ion-exchange resin was added. The slurry was gently stirred for 17 h, and, afterward, the resin was removed using vacuum filtration and the solution was concentrated using rotary evaporation. ³¹P NMR can be used to monitor the disappearance of the PF₆⁻ anion; if the exchange is incomplete, resin and solvent can be re-added to the product to continue the exchange process. The resulting oil was dissolved in 25 mL of CH₂Cl₂ and washed twice with 15 mL of brine solution. The organic layer was concentrated, and the crude solid was further dried under vacuum (60 mTorr) at 60 °C for 3 h. The resulting white solid was analyzed by ³¹P{¹H} to ensure full conversion to the Cl⁻ form. CyMe[Cl] $^{31}P\{^{1}H\}$ NMR (202 MHz, CDCl₃) δ 46.7. **iPrMe**[CI] $^{31}P\{^{1}H\}$ NMR (202 MHz, CDCl₂) δ 45.0.

Homopolymerization of CyMe[CI] Using Ring-Opening Metathesis Polymerization. G3 (2.0 mg, 0.0027 mmol) and 0.4 mL of dichloroethane were added to a 20 mL scintillation vial equipped with a septum-sealed cap in a glovebox with a nitrogen atmosphere. In a separate vial, CyMe[Cl] (148 mg, 0.3 mmol) was dissolved in 1.0 mL of dichloroethane and this solution was rapidly injected into the initiator solution at 22 °C and the reaction mixture was stirred for 45 min. The polymerization was quenched by rapidly injecting 0.5 mL (5.2 mmol) of ethyl vinyl ether and stirring for 30 min. The remaining solvent was concentrated to approximately 1 mL, and this solution was precipitated into 50 mL of diethyl ether. The solids were collected using vacuum filtration (143 mg, 97% yield).

General Stat hPN-co-Phos Procedure. G3 (2.0 mg, 0.0027 mmol) was dissolved in 4.9 mL of chlorobenzene in a 20 mL scintillation vial equipped with a septum-sealed cap in a glovebox with a nitrogen atmosphere (O₂ < 0.1 ppm). In a separate vial, the phosphonium monomer (0.23, or 0.19 mmol) and norbornene (1.14, or 1.18 mmol) were dissolved in 2.0 mL of chlorobenzene and this solution was rapidly injected into the initiator solution at 22 °C. The reaction mixture was stirred for 45 min and then was quenched by rapidly injecting 1.0 mL (10.4 mmol) of ethyl vinyl ether followed by stirring for 30 min. A 0.1 mL aliquot was removed and analyzed using GPC and NMR spectroscopy. The remaining solvent was concentrated to approximately 0.5 mL using rotary evaporation, and this solution was precipitated into 25 mL of diethyl ether. The polymer was hydrogenated to produce a white solid (70-90% yield).

General hPN-b-Phos Procedure. G3 (2.0 mg, 0.0027 mmol) was dissolved in 4.6 mL of chlorobenzene in a 20 mL scintillation vial equipped with a septum-sealed cap in a glovebox with a nitrogen atmosphere ($O_2 < 0.1$ ppm) and the solution was cooled to -10 °C using an ice/salt bath. In a separate vial, norbornene (104 mg, 1.1 mmol) was dissolved in 1.0 mL of chlorobenzene and this was rapidly injected into the initiator solution. The reaction mixture was stirred for 20 min, and then a 0.1 mL aliquot was removed, quenched with ethyl vinyl ether, and analyzed using GPC and NMR spectroscopy. The phosphonium monomer (0.27 mmol) was dissolved in 1.3 mL of

chlorobenzene and was rapidly injected into the polymer solution. The polymerization was immediately removed from the -10 °C bath and warmed to room temperature. After 45 min, the polymerization was quenched with 1.0 mL (10.4 mmol) of ethyl vinyl ether. A 0.1 mL aliquot was removed and analyzed using GPC and NMR spectroscopy. The remaining solvent was concentrated to approximately 0.5 mL using rotary evaporation, and this solution was precipitated into 25 mL of diethyl ether. The polymer was hydrogenated to produce a tan solid (70% yield).

General Polymer Hydrogenation Procedure. In a 25 mL flask equipped with a reflux condenser, the polymer (250 mg) was dissolved in chlorobenzene (15 mL). Tripropylamine (2.1 mL, 11 mmol) and p-toluenesulfonyl hydrazide (0.51 g, 2.7 mmol) were added, and the reaction mixture was heated to 125 °C using an oil bath. After 2 h, the contents of the flask were cooled to room temperature and the mixture was precipitated into 100 mL of diethyl ether. The solids were filtered off and soaked in 20 mL of 1:3 MeOH/ sat. sodium bicarbonate solution at 80 $^{\circ}$ C for 3–4 h. The polymer was removed by vacuum filtration, rinsed with water, and dried in vacuo at 80 °C for 8 h. The extent of hydrogenation was determined from ¹H NMR analysis by loss of the vinyl signals (5.36 ppm, 5.21 ppm). If polymerized in the PF₆⁻ form, the solids were dissolved in 1:2 TCE/ MeOH and exchanged to the Cl⁻ form using an Amberlite IRA-400 Cl Exchange Resin.

Representative Set of NMR Signals for the Stat Copolymers. 5:1 Stat hPN-CyMe[Cl]. ¹H NMR (500 MHz, TCE- d_2) δ 3.06-2.83 (m, 4H), 2.80-2.65 (m, 3H), 2.65-2.50 (m, 9H), 2.11-1.98 (m, 2H), 1.98-1.86 (m, 11H), 1.86-1.47 (m, 38H), 1.41-1.01 (m, 40H), 0.88–0.72 (m, 1H), 0.62 (q, J = 10.3 Hz, 4H). $^{13}C\{^{1}H\}$ NMR (126 MHz, TCE- d_2) δ 55.7, 54.0 (br), 40.6, 40.2, 35.6, 35.2, 31.6, 30.4, 29.8, 25.9, 24.8. $^{31}P\{^{1}H\}$ NMR (202 MHz, TCE- d_2) δ 46.1-45.0. Two notes for the NMR signals of stat 5:1 hPN-CyMe: the signal reported at 3.06-2.83 integrates 1H lower than expected. The aliphatic region integrates to within 10% of expected relative to the N-Me protons. These should be \sim 101H and integrate to \sim 95H. 5:1 Stat hPN-iPrMe[Cl]. 1 H NMR (500 MHz, TCE- d_2) δ 3.54– 3.38 (m, 3H), 3.13-2.85 (m, 1H), 2.80-2.65 (m, 3H), 2.65-2.47 (m, 9H), 2.11-2.00 (m, 1H), 1.99-1.85 (m, 6H), 1.84-1.60 (m, 19H), 1.45-1.03 (m, 48H), 1.03-0.69 (m, 1H), 0.61 (q, J = 10.3 Hz, 4H). 13 C{ 1 H} NMR (126 MHz, TCE- d_2) δ 53.7 (br), 47.0, 40.6, 40.2, 35.6, 35.2, 31.6, 29.6, 28.4, 19.9. ³¹P{¹H} NMR (202 MHz, TCE-d₂) δ 45.7–44.4. Two notes for the NMR signals of stat 5:1 hPN-iPrMe: the signal reported at 3.13-2.85 integrates 1H lower than expected. The aliphatic region integrates to within 10% of expected relative to the N-Me protons. These should be ~89H and integrate to ~79H.

ASSOCIATED CONTENT

Supporting Information

The Supporting Information is available free of charge at https://pubs.acs.org/doi/10.1021/acs.macromol.0c00422.

GPC chromatograms of polymers, NMR spectra, Nyquist plots, high-resolution mass spectrometry, photos of copolymers, and thermal analysis (PDF)

AUTHOR INFORMATION

Corresponding Authors

Tomasz Kowalewski - Department of Chemistry, Carnegie Mellon University, Pittsburgh, Pennsylvania 15213-2617, *United States;* orcid.org/0000-0002-3544-554X;

Email: tomek@andrew.cmu.edu

Kevin J. T. Noonan – Department of Chemistry, Carnegie Mellon University, Pittsburgh, Pennsylvania 15213-2617, *United States;* • orcid.org/0000-0003-4061-7593; Email: noonan@andrew.cmu.edu

Authors

- Megan Treichel Department of Chemistry, Carnegie Mellon University, Pittsburgh, Pennsylvania 15213-2617, United States
- C. Tyler Womble Department of Chemistry, Carnegie Mellon University, Pittsburgh, Pennsylvania 15213-2617, United States; © orcid.org/0000-0003-4890-4351
- Ryan Selhorst Department of Chemistry, Carnegie Mellon University, Pittsburgh, Pennsylvania 15213-2617, United States
- Jamie Gaitor Department of Chemistry, Carnegie Mellon University, Pittsburgh, Pennsylvania 15213-2617, United States
- **Taniya M. S. K. Pathiranage** Department of Chemistry, Carnegie Mellon University, Pittsburgh, Pennsylvania 15213-2617, United States

Complete contact information is available at: https://pubs.acs.org/10.1021/acs.macromol.0c00422

Notes

The authors declare no competing financial interest.

ACKNOWLEDGMENTS

K.J.T.N. and T.K. are grateful to the NSF for support of this work (CHE-1809658). Minjung Lee (UMass Amherst), Ryan Hayward (UMass Amherst), and Doowon Lee (University of Pittsburgh) are acknowledged for help with small-angle X-ray scattering experiments. Brian Long (University of Tennessee) is acknowledged for helpful discussions. Terry Collins is acknowledged for help with pH measurements.

REFERENCES

- (1) Tanaka, Y. Ion Exchange Membranes: Fundamentals and Applications, 1st ed.; Elsevier: Amsterdam, Boston, 2007; p 531.
- (2) You, W.; Noonan, K. J. T.; Coates, G. W. Alkaline-Stable Anion Exchange Membranes: A Review of Synthetic Approaches. *Prog. Polym. Sci.* **2020**, *100*, 101177.
- (3) Noh, S.; Jeon, J. Y.; Adhikari, S.; Kim, Y. S.; Bae, C. Molecular Engineering of Hydroxide Conducting Polymers for Anion Exchange Membranes in Electrochemical Energy Conversion Technology. *Acc. Chem. Res.* **2019**, *52*, 2745–2755.
- (4) Arges, C. G.; Zhang, L. Anion Exchange Membranes' Evolution toward High Hydroxide Ion Conductivity and Alkaline Resiliency. *ACS Appl. Energy Mater.* **2018**, *1*, 2991–3012.
- (5) Varcoe, J. R.; Atanassov, P.; Dekel, D. R.; Herring, A. M.; Hickner, M. A.; Kohl, P. A.; Kucernak, A. R.; Mustain, W. E.; Nijmeijer, K.; Scott, K.; Xu, T.; Zhuang, L. Anion-Exchange Membranes in Electrochemical Energy Systems. *Energy Environ. Sci.* **2014**, *7*, 3135–3191.
- (6) Hickner, M. A.; Herring, A. M.; Coughlin, E. B. Anion Exchange Membranes: Current Status and Moving Forward. *J. Polym. Sci. Part B: Polym. Phys.* **2013**, *51*, 1727–1735.
- (7) Noonan, K. J. T.; Hugar, K. M.; Kostalik, H. A.; Lobkovsky, E. B.; Abruña, H. D.; Coates, G. W. Phosphonium-Functionalized Polyethylene: A New Class of Base-Stable Alkaline Anion Exchange Membrane. *J. Am. Chem. Soc.* **2012**, *134*, 18161–18164.
- (8) Womble, C. T.; Coates, G. W.; Matyjaszewski, K.; Noonan, K. J. T. Tetrakis(dialkylamino)phosphonium Polyelectrolytes Prepared by Reversible Addition-Fragmentation Chain Transfer Polymerization. *ACS Macro Lett.* **2016**, *5*, 253–257.
- (9) You, W.; Hugar, K. M.; Coates, G. W. Synthesis of Alkaline Anion Exchange Membranes with Chemically Stable Imidazolium Cations: Unexpected Cross-Linked Macrocycles from Ring-Fused ROMP Monomers. *Macromolecules* **2018**, *51*, 3212–3218.

- (10) Disabb-Miller, M. L.; Zha, Y.; DeCarlo, A. J.; Pawar, M.; Tew, G. N.; Hickner, M. A. Water Uptake and Ion Mobility in Cross-Linked Bis(terpyridine)ruthenium-Based Anion Exchange Membranes. *Macromolecules* **2013**, *46*, 9279–9287.
- (11) Zha, Y.; Disabb-Miller, M. L.; Johnson, Z. D.; Hickner, M. A.; Tew, G. N. Metal-Cation-Based Anion Exchange Membranes. *J. Am. Chem. Soc.* **2012**, *134*, 4493–4496.
- (12) Kostalik, H. A.; Clark, T. J.; Robertson, N. J.; Mutolo, P. F.; Longo, J. M.; Abruña, H. D.; Coates, G. W. Solvent Processable Tetraalkylammonium-Functionalized Polyethylene for Use as an Alkaline Anion Exchange Membrane. *Macromolecules* **2010**, *43*, 7147–7150.
- (13) Robertson, N. J.; Kostalik, H. A.; Clark, T. J.; Mutolo, P. F.; Abruña, H. D.; Coates, G. W. Tunable High Performance Cross-Linked Alkaline Anion Exchange Membranes for Fuel Cell Applications. *J. Am. Chem. Soc.* **2010**, *132*, 3400–3404.
- (14) Clark, T. J.; Robertson, N. J.; Kostalik, H. A.; Lobkovsky, E. B.; Mutolo, P. F.; Abruña, H. D.; Coates, G. W. A Ring-Opening Metathesis Polymerization Route to Alkaline Anion Exchange Membranes: Development of Hydroxide-Conducting Thin Films from an Ammonium-Functionalized Monomer. J. Am. Chem. Soc. 2009, 131, 12888–12889.
- (15) Zhu, T.; Xu, S.; Rahman, A.; Dogdibegovic, E.; Yang, P.; Pageni, P.; Kabir, M. P.; Zhou, X.-d.; Tang, C. Cationic Metallo-Polyelectrolytes for Robust Alkaline Anion-Exchange Membranes. *Angew. Chem., Int. Ed.* **2018**, *57*, 2388–2392.
- (16) Zhu, T.; Sha, Y.; Firouzjaie, H. A.; Peng, X.; Cha, Y.; Dissanayake, D. M. M. M.; Smith, M. D.; Vannucci, A. K.; Mustain, W. E.; Tang, C. Rational Synthesis of Metallo-Cations Toward Redoxand Alkaline-Stable Metallo-Polyelectrolytes. *J. Am. Chem. Soc.* **2020**, 142, 1083–1089.
- (17) Chen, W.; Mandal, M.; Huang, G.; Wu, X.; He, G.; Kohl, P. A. Highly Conducting Anion-Exchange Membranes Based on Cross-Linked Poly(norbornene): Ring Opening Metathesis Polymerization. ACS Appl. Energy Mater. 2019, 2, 2458–2468.
- (18) Price, S. C.; Ren, X.; Savage, A. M.; Beyer, F. L. Synthesis and Characterization of Anion-Exchange Membranes Based on Hydrogenated Poly(norbornene). *Polym. Chem.* **2017**, *8*, 5708–5717.
- (19) Ishikawa, T. Superbases for Organic Synthesis: Guanidines, Amidines, Phosphazenes and Related Organocatalysts; Wiley: Chichester, West Sussex, U.K., 2009; p 326.
- (20) Schwesinger, R.; Link, R.; Wenzl, P.; Kossek, S.; Keller, M. Extremely Base-Resistant Organic Phosphazenium Cations. *Chem. Eur. J.* **2006**, *12*, 429–437.
- (21) Womble, C. T.; Kang, J.; Hugar, K. M.; Coates, G. W.; Bernhard, S.; Noonan, K. J. T. Rapid Analysis of Tetrakis-(dialkylamino)phosphonium Stability in Alkaline Media. *Organometallics* **2017**, *36*, 4038–4046.
- (22) Marchenko, A. P.; Koidan, G. N.; Pinchuk, A. M. Interaction of Tetrakis(Dialkylamido)Phosphoniumbromides with Bases. *Russ. J. Gen. Chem.* **1984**, *54*, 2405–2409.
- (23) Lee, L.-B. W.; Register, R. A. Hydrogenated Ring-Opened Polynorbornene: A Highly Crystalline Atactic Polymer. *Macromolecules* **2005**, *38*, 1216–1222.
- (24) Cataldo, F. FTIR Spectroscopic Characterization of Hydrogenated Polyoctenamer and Polynorbornene and DSC Study of Their Thermal-Properties. *Polym. Int.* **1994**, *34*, 49–57.
- (25) Barnes, A. M.; Du, Y.; Liu, B.; Zhang, W.; Seifert, S.; Coughlin, E. B.; Buratto, S. K. Effect of Surface Alignment on Connectivity in Phosphonium-Containing Diblock Copolymer Anion-Exchange Membranes. J. Phys. Chem. C 2019, 123, 30819–30826.
- (26) Zhang, W.; Liu, Y.; Jackson, A. C.; Savage, A. M.; Ertem, S. P.; Tsai, T. H.; Seifert, S.; Beyer, F. L.; Liberatore, M. W.; Herring, A. M.; Coughlin, E. B. Achieving Continuous Anion Transport Domains Using Block Copolymers Containing Phosphonium Cations. *Macromolecules* **2016**, *49*, 4714–4722.
- (27) Zhang, B.; Kaspar, R. B.; Gu, S.; Wang, J.; Zhuang, Z.; Yan, Y. A New Alkali-Stable Phosphonium Cation Based on Fundamental

- Understanding of Degradation Mechanisms. ChemSusChem 2016, 9, 2374-2379.
- (28) Gu, S.; Cai, R.; Yan, Y. Self-Crosslinking for Dimensionally Stable and Solvent-Resistant Quaternary Phosphonium Based Hydroxide Exchange Membranes. *Chem. Commun.* **2011**, 47, 2856–2858
- (29) Gu, S.; Cai, R.; Luo, T.; Jensen, K.; Contreras, C.; Yan, Y. S. Quaternary Phosphonium-Based Polymers as Hydroxide Exchange Membranes. *ChemSusChem* **2010**, *3*, 555–558.
- (30) Gu, S.; Cai, R.; Luo, T.; Chen, Z.; Sun, M.; Liu, Y.; He, G.; Yan, Y. A Soluble and Highly Conductive Ionomer for High-Performance Hydroxide Exchange Membrane Fuel Cells. *Angew. Chem., Int. Ed.* **2009**, *48*, 6499–6502.
- (31) Schwesinger, R.; Willaredt, J.; Schlemper, H.; Keller, M.; Schmitt, D.; Fritz, H. Novel, Very Strong, Uncharged Auxiliary Bases; Design and Synthesis of Monomeric and Polymer-Bound Triaminoi-minophosphorane Bases of Broadly Varied Steric Demand. *Chem. Ber.* **1994**, *127*, 2435–2454.
- (32) Womble, C. T. Synthesis, Characterization, and Polymerization of Tetrakis(dialkylamino)phosphonium Cations. Dissertation, Carnegie Mellon: Pittsburgh, PA, 2018.
- (33) Radzinski, S. C.; Foster, J. C.; Matson, J. B. Preparation of Bottlebrush Polymers via a One-Pot Ring-Opening Polymerization (ROP) and Ring-Opening Metathesis Polymerization (ROMP) Grafting-Through Strategy. *Macromol. Rapid Commun.* **2016**, 37, 616–621.
- (34) Manning, D. D.; Strong, L. E.; Hu, X.; Beck, P. J.; Kiessling, L. L. Neoglycopolymer Inhibitors of the Selectins. *Tetrahedron* **1997**, 53, 11937–11952.
- (35) Berson, J. A.; Ben-Efraim, D. A. Resolution, Stereochemial Correlation and Maximum Rotations of the Norbornane- and 5-Norbornene-2-Carboxylic Acids. Isotope Dilution as an Aid in the Determination of Optical Purity. *J. Am. Chem. Soc.* **1959**, *81*, 4083–4087.
- (36) Choi, T.-L.; Grubbs, R. H. Controlled Living Ring-Opening-Metathesis Polymerization by a Fast-Initiating Ruthenium Catalyst. *Angew. Chem., Int. Ed.* **2003**, 42, 1743–1746.
- (37) Bielawski, C. W.; Grubbs, R. H. Living Ring-Opening Metathesis Polymerization. *Prog. Polym. Sci.* **2007**, *32*, 1–29.
- (38) He, H.; Zhong, M.; Adzima, B.; Luebke, D.; Nulwala, H.; Matyjaszewski, K. A Simple and Universal Gel Permeation Chromatography Technique for Precise Molecular Weight Characterization of Well-Defined Poly(ionic liquid)s. J. Am. Chem. Soc. 2013, 135, 4227–4230.
- (39) Elabd, Y. A.; Hickner, M. A. Block Copolymers for Fuel Cells. *Macromolecules* **2011**, *44*, 1–11.
- (40) Shin, D. W.; Guiver, M. D.; Lee, Y. M. Hydrocarbon-Based Polymer Electrolyte Membranes: Importance of Morphology on Ion Transport and Membrane Stability. *Chem. Rev.* **2017**, *117*, 4759–4805.
- (41) Mohanty, A. D.; Ryu, C. Y.; Kim, Y. S.; Bae, C. Stable Elastomeric Anion Exchange Membranes Based on Quaternary Ammonium-Tethered Polystyrene-b-poly(ethylene-co-butylene)-b-polystyrene Triblock Copolymers. *Macromolecules* **2015**, *48*, 7085–7095.
- (42) Vezzù, K.; Maes, A. M.; Bertasi, F.; Motz, A. R.; Tsai, T.-H.; Coughlin, E. B.; Herring, A. M.; Di Noto, V. Interplay Between Hydroxyl Density and Relaxations in Poly-(vinylbenzyltrimethylammonium)-b-poly(methylbutylene) Membranes for Electrochemical Applications. J. Am. Chem. Soc. 2018, 140, 1372–1384.
- (43) Li, Y.; Liu, Y.; Savage, A. M.; Beyer, F. L.; Seifert, S.; Herring, A. M.; Knauss, D. M. Polyethylene-Based Block Copolymers for Anion Exchange Membranes. *Macromolecules* **2015**, *48*, 6523–6533.
- (44) Miyanishi, S.; Fukushima, T.; Yamaguchi, T. Synthesis and Property of Semicrystalline Anion Exchange Membrane with Well-Defined Ion Channel Structure. *Macromolecules* **2015**, *48*, 2576–2584.

- (45) You, W.; Padgett, E.; MacMillan, S. N.; Muller, D. A.; Coates, G. W. Highly conductive and chemically stable alkaline anion exchange membranes via ROMP of *trans*-cyclooctene derivatives. *Proc. Natl. Acad. Sci. U.S.A.* **2019**, *116*, 9729–9734.
- (46) Lin, B.; Xu, F.; Su, Y.; Zhu, Z.; Ren, Y.; Ding, J.; Yuan, N. Facile Preparation of Anion-Exchange Membrane Based on Polystyrene-b-polybutadiene-b-polystyrene for the Application of Alkaline Fuel Cells. *Ind. Eng. Chem. Res.* **2019**, *58*, 22299–22305.
- (47) Lin, C. X.; Wu, H. Y.; Li, L.; Wang, X. Q.; Zhang, Q. G.; Zhu, A. M.; Liu, Q. L. Anion Conductive Triblock Copolymer Membranes with Flexible Multication Side Chain. *ACS Appl. Mater. Interfaces* **2018**, *10*, 18327–18337.
- (48) Liu, L.; Ahlfield, J.; Tricker, A.; Chu, D.; Kohl, P. A. Anion Conducting Multiblock Copolymer Membranes with Partial Fluorination and Long Head-Group Tethers. *J. Mater. Chem. A* **2016**, *4*, 16233–16244.
- (49) Weiber, E. A.; Meis, D.; Jannasch, P. Anion conducting multiblock poly(arylene ether sulfone)s containing hydrophilic segments densely functionalized with quaternary ammonium groups. *Polym. Chem.* **2015**, *6*, 1986–1996.
- (50) Park, D. Y.; Kohl, P. A.; Beckham, H. W. Anion-Conductive Multiblock Aromatic Copolymer Membranes: Structure-Property Relationships. *J. Phys. Chem. C* **2013**, *117*, 15468–15477.
- (51) Zhao, Z.; Wang, J.; Li, S.; Zhang, S. Synthesis of multi-block poly(arylene ether sulfone) copolymer membrane with pendant quaternary ammonium groups for alkaline fuel cell. *J. Power Sources* **2011**, *196*, 4445–4450.
- (52) Tanaka, M.; Fukasawa, K.; Nishino, E.; Yamaguchi, S.; Yamada, K.; Tanaka, H.; Bae, B.; Miyatake, K.; Watanabe, M. Anion Conductive Block Poly(arylene ether)s: Synthesis, Properties, and Application in Alkaline Fuel Cells. *J. Am. Chem. Soc.* **2011**, *133*, 10646–10654.
- (53) Buggy, N. C.; Du, Y.; Kuo, M.-C.; Ahrens, K. A.; Wilkinson, J. S.; Seifert, S.; Coughlin, E. B.; Herring, A. M. A Polyethylene-Based Triblock Copolymer Anion Exchange Membrane with High Conductivity and Practical Mechanical Properties. *ACS Appl. Polym. Mater.* **2020**, *2*, 1294–1303.
- (54) Mandal, M.; Huang, G.; Kohl, P. A. Anionic Multiblock Copolymer Membrane Based on Vinyl Addition Polymerization of Norbornenes: Applications in Anion-Exchange Membrane Fuel Cells. *J. Membr. Sci.* **2019**, *570–571*, 394–402.
- (55) Mandal, M.; Huang, G.; Kohl, P. A. Highly Conductive Anion-Exchange Membranes Based on Cross-Linked Poly(norbornene): Vinyl Addition Polymerization. *ACS Appl. Energy Mater.* **2019**, *2*, 2447–2457.
- (56) Montanari, F.; Landini, D.; Rolla, F. Phase-Transfer Catalyzed Reactions. *Top. Curr. Chem.* **1982**, *101*, 147–200.
- (57) Fawcett, A. H. *Polymer Spectroscopy*; Wiley: Chichester, England, 1996; p 393.
- (58) Ai-Samak, B.; Amir-Ebrahimi, V.; Carvill, A. G.; Hamilton, J. G.; Rooney, J. J. Determination of the Tacticity of Ring-Opened Metathesis Polymers of Norbornene and Norbornadiene by ¹³C NMR Spectroscopy of Their Hydrogenated Derivatives. *Polym. Int.* **1996**, *41*, 85–92.
- (59) Roe, R. J. Methods of X-Ray and Neutron Scattering in Polymer Science; Oxford University Press: New York, 2000; p 331.
- (60) Sanford, M. S.; Love, J. A.; Grubbs, R. H. A Versatile Precursor for the Synthesis of New Ruthenium Olefin Metathesis Catalysts. *Organometallics* **2001**, *20*, 5314–5318.
- (61) Harris, R. K.; Becker, E. D.; De Menezes, S. M. C.; Goodfellow, R.; Granger, P. NMR nomenclature. Nuclear spin properties and conventions for chemical shifts (IUPAC recommendations 2001). *Pure Appl. Chem.* **2001**, *73*, 1795–1818.